Geotechnical and Geophysical Site Characterisation 5 – Lehane, Acosta-Martínez & Kelly (Eds)

Integrated use of terrestrial laser scanning and thermal imagery for characterization of hydrothermally altered granites

J.S. Coggan, D.M. Pascoe, & M.L.Eyre
University of Exeter, Cornwall, UK

J.H.Howe
IMERYS Minerals Ltd, Cornwall UK

ABSTRACT: The assessment of material properties is a fundamental component of geotechnical characterization of slopes in hydrothermally altered granite, as potential slope failure mechanisms are controlled by kaolinization intensity, discontinuity characteristics (such as orientation, persistence and spacing) and the detrimental effects of groundwater. In order to assess the potential advantages of remote mapping technologies for improved spatial cover both laser scanning and photogrammetry have been evaluated within the china clay operations for use in rock mass characterization. The results presented also focus on application of the remotely captured data for use in design of china clay slopes in southwest England. A key benefit of the detailed geo-referenced point cloud data is the ability to measure and evaluate discontinuity characteristics such as orientation, spacing, persistence and volumetric data which are key factors that dictate the size of any potential failure. In addition to capturing rock mass characteristics, accurate slope geometries and digital terrain models can be derived for more effective slope management. Through use of photo-overlays and coloured point cloud data captured from use of terrestrial laser scanning, based on red green blue (RGB) values, it was also possible to evaluate discontinuity type, such as tourmaline veins within the point cloud. Integration of laser scanning derived data with overlays from infra red and thermal images was also performed to assist identification of alteration zones within a slope. The results highlight the benefits of using remote mapping technologies for rock mass characterization and acquisition of spatial data for planning purposes.

1 INTRODUCTION

1.1 *Geological Setting*

Kaolinized china clay areas of the granite batholith can be found in Cornwall, including the centrally positioned deposits in St Austell. The long history of china clay extraction, since deposits were first discovered by William Cookworthy in 1746, has left a legacy of historical pit faces which were designed prior to the Quarry Regulations (Health and Safety Executive, 2013).

This paper discusses the combination of 3-D laser scanning and thermal infrared imaging which was used to map historic bench faces in the china clay pits to provide input parameters for rock mass characterisation to allow slope stability analyses to be carried out.

1.2 *Kaolinization of Granite*

Kaolin (china clay) is produced by the alteration of granite, through the interaction of hydrothermal fluids and groundwater with feldspar causing hydrothermal decomposition to form kaolinite (Wilson, 2006).

Lower temperature (<100ºC) high salinity hydrothermal fluids also played a major role in the kaolinization process (Psyrillos *et al*., 1998; Manning *et al*., 1996) also indicated that meteoric water was also involved. It is also considered that both hydrothermal and low-temperature weathering processes were contributing factors (Bristow and Exley, 1994). The grading system for the china clay deposits in Cornwall used by Imerys is shown in Table 1.

In lower grades of kaolinized granite, in particular Grades II and III, slope failures are most likely to be kinematically controlled by discontinuities within the rock mass, causing wedge, toppling and plane failure along with general rockfall from the bench crests. Rock fall due to unfavourably aligned joint surfaces in a higher bench may affect development at lower levels towards the toe of the slope. Rock-trap design to overcome this safety risk is of great importance.

In more highly kaolinized granite (Grades IV and V), rotational failures through the body of the rock are more likely and require continuum modelling of

slope stability, although relict discontinuities can still have an effect. Thus the degree of kaolinization highly influences the design of pit slopes, with overall slope angles in highly kaolinized zones being as low as 25 degrees.

Table 1. China clay grading (altered from Stead et al. 2000)

Grade	Description	Characteristics	Geological hammer blows (break)	Unconfined Compressive Strength (UCS) values based on Schmidt hammer rebound value
I	Fresh rock	No visible alteration	Multiple	n/a
II	Slightly altered	Slight discolouration and weakening	More than one	>45 MPa
III	Moderately altered	Considerable weakening, penetrative discolouration	Single	25-45 MPa
IV	Highly altered	Large pieces broken by hand	n/a	0-25 MPa
V	Completely altered	Considerably weakened, original texture preserved, slakes readily in water	Geological pick penetrates	50-250 kPa
VI	Residual soil	Soil mixture with no rock	n/a	<50 kPa

In less kaolinized zones, individual benches can be near vertical as demonstrated in Figure 1, where the slope of this historic bench face is approximately 26 m high at an inclination of 80+/-5 degrees with significant rock traps constructed to manage risk. Also shown in the photograph is the presence of several narrow highly kaolinized zones within this mostly poorly kaolinized bench face which have been oriented using remote methods, as described in this paper.

Figure 1. Photograph of a section of historical bench face (striking N-S) with several sub-vertical kaolinized zones, found within poorly kaolinized rock. Discontinuities sets of high angle joints striking sub parallel to the face subject to possible toppling failure.

2 STRUCTURAL ORIENTATIONS

Tectonic, lithostatic and thermal stresses and pore pressures set up strain in rock leading to the formation of discontinuities. Stead *et al.*, (2000) reported that the kaolinization in the St. Austell granite is structurally controlled and generally occurs in association with greisen, tourmaline and quartz veining. The kaolinized zones are often orientated parallel to NW-SE and ENE-WSW striking structures due to the in-situ stresses at the time of formation. NNW-SSE trending wrench faults known as cross courses also occur throughout the Cornubian orefield. Some of the outcropping kaolinized zones are up to several hundreds of metres across and tend to be funnel-shaped or trough-like in cross section, narrowing downwards with stems more than 300m below surface. An understanding of these structural controls on discontinuities and alteration grade, can be gained using remote sensing methods required to enable safe slope design.

2.1 *Remote Sensing*

The excavated slopes investigated within the china clay area, exhibit various levels of stability, making direct access to the faces unattainable. This inaccessibility necessitates the use of remote sensing, preferably using a combination of methods: 3-D laser scanning and thermal infrared imaging as described in this paper.

2.2 *3-D Laser Scanning*

Terrestrial LiDAR scanners are based on electromagnetic distance measurement. Using the known constant speed of light, the range to the target can be calculated. In addition, angular measurement is also obtained electronically. Multiple scans from different locations along the slope face minimized the blinding effect (occlusion) of a single line of sight (Sturzenegger and Stead, 2009). The individual scans were joined together in Cyclone software to produce the combined image in Figure 2 (consisting of 20 million points). The point cloud was split vertically into five sections to speed the processing in Split-FX software (Split-FX, 2013) which was used to analyse the three dimensional point cloud data.

The laser scan in Figure 2 shows the coloured point cloud based on the RGB (red, green, blue) values. This technique has the potential for a further degree of identification of discontinuity type – vein, joint, fault etc. For instance, the tourmalinized joints can be picked out by their dark grey/black colouration.

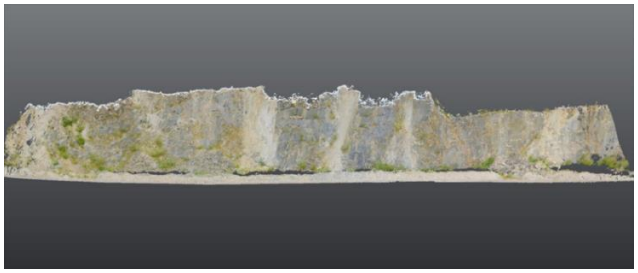

Figure 2. Coloured point cloud of an historic excavated face in a china clay pit

2.3 *Analysis of point clouds using Split FX software*

Point cloud data was imported into Split-FX software, to enable the orientation of discontinuities to be identified. Zones where no patches could be fitted

corresponded mostly with highly altered zones where the joints have been obscured by the process of kaolinization. Where discontinuities were striking almost perpendicular to the bench face it was not always possible to fit patches to the surface of the discontinuity and 'traces' were fitted, enabling orientation of these joints to be determined as demonstrated in Figure 3.

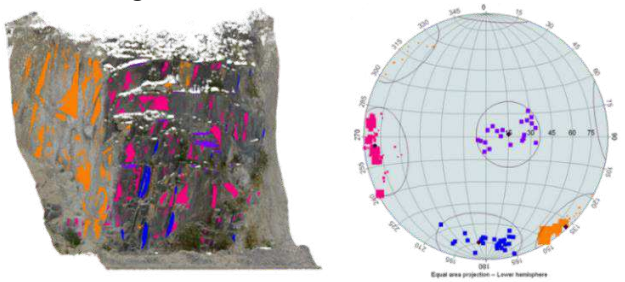

(a) (b)

Figure 3. a) 3-D laser scan of section of pit benches indicating patches (angular) and traces (ovoid) added b) Stereoplot of section of NE face pit bench indicating poles of patches (angular) and traces (ovoid) with each joint set colour-coded.

Orientation data for each of the major sets identified in each of the four sections of the slope are shown in Table 2.

Table 2. Orientation data for major joint sets in 5 sections of the bench.

Set number	Dip	Dip Direction	Fisher K
1	81	082	134.5
2	86	310	154.9
3	77	348	147.8
4	18	251	47.9

The major planes plot indicates the average pole for each set identified from cluster data and these results are given in Table 3. Contouring is enabled in Dips using the "floating cone" method in which pole counting is done on the 3-D sphere. Fisher's constant (K), which gives some measure of the degree of clustering in a given set.

Dominant joint set 1 is preferentially sampled as it strikes almost parallel to the bench face, dipping into the slope face at 81 degrees towards 082°. Set 4 is nearly horizontal and has the lowest k value.

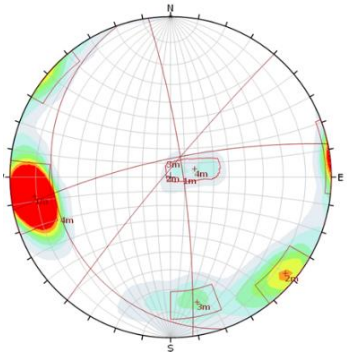

Figure 4. Contoured lower hemisphere equal angle stereographic projection of discontinuities in combined sections 1- 5.

Table 3. Mean poles of major joint sets and Fisher constants in east face of Melbur Pit

Section	Set 1 (pink) Orientation (Dip/Dip Dir.)	Set 2 (orange) Orientation (Dip/Dip Dir.)	Set 3 (blue) Orientation (Dip/Dip Dir.)	Set 4 (purple) Orientation (Dip/Dip Dir.)
1	82/076	88/298	79/007	05/257
2	77/083	78/304	74/355	14/270
3	77/082	87/317	75/004	15/264
4	85/078	84/316	70/355	21/267
5	74/073	84/294	79/344	14/241

It is also possible to determine estimates of the true spacing and persistence of discontinuities using Split-FX, achieved by measuring the perpendicular distance between fitted traces and patches. The probability density distributions of both total discontinuity lengths and spacings are shown in Figure 5. Individual joint set spacings from sections 2, 3 and 4 are presented in Table 4.

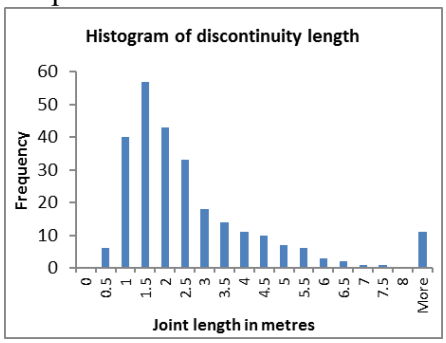

Figure 5. Histogram of discontinuity length.

Table 4. Mean poles of major joint sets and Fisher constants in east face of Melbur Pit

Set 1 (pink)				
	Spacing			
Section	Mean	Maximum	Minimum	Standard deviation
1	0.7	2.37	0.15	0.54
2	0.47	1.06	0.11	0.29
3	0.64	1.54	0.24	0.4
4	0.5	1.27	0.07	0.3
Set 2 (orange)				
	Spacing			
Section	Mean	Maximum	Minimum	Standard deviation
1	0.91	1.8	0.22	0.47
2	1.31	2.21	0.59	0.53
3	1.12	3.92	0.12	1.1
4	1.07	2.06	0.23	0.57
Set 3 (blue)				
	Spacing			
Section	Mean	Maximum	Minimum	Standard deviation
1	1.24	2.47	0.46	0.63
2	1.13	2.25	0.44	0.53
3	2.41	5.8	0.26	1.41
4	0.94	1.67	0.34	0.44
Set 4 (purple)				
	Spacing			
Section	Mean	Maximum	Minimum	Standard deviation
1	0.84	1.73	0.23	0.39
2	0.68	1.25	0.25	0.33
3	1.67	3.99	0.21	1.25
4	1.69	3.09	0.79	0.62

Measurements of true persistence were exported directly from Split-FX, shown in Table 5. It can be seen, traces in section 2 appear to be approximately twice as long as in the other sections. Upon reviewing the point clouds data there are two very long individual traces of 20.8 and 24.41m listed which skew the data.

Table 5. True trace lengths exported from sections of NE face of Melbur Pit.

Section	Mean true lengths	Standard deviation
1	1.83	1.33
2	4.02	4.6
3	2.27	2.01
4	2.50	1.86
5	2.47	2.49

2.4 *Kinematic Analysis*

Based on the data described above, the preliminary kinematic analysis which quantifies the likelihood of plane, wedge and toppling failures was carried out for the east face of the pit and the results are shown in Figure 6 (a)-(d) where the pink shaded areas identify the critical sets or intersections of joint sets for each failure mode.

Kinematically, the opportunities for both direct/oblique and flexural toppling failures are predominant with planar and wedge failure being much less significant. Input data included a slope dip of 70, dip direction of slope of 270° and angle of internal friction of 30°. As seen in Figure 6(a), plane failure analysis indicated that of the 796 discontinuities created by fitting patches and traces to the point cloud, only 15 (1.9%) were deemed critical. Figure 6(b) shows there is a low possibility of wedge failure with an estimated 4.3% of joint intersections being classified as critical due to them daylighting in the slope and the chosen friction angle of 30° exceeded. For direct toppling, including oblique toppling to occur, high angle joints dipping into the slope face are required plus an intersection with another high angle joint set, to form the vertical slabs. Of a possible total of 316,180 intersections 5.2% were critical. For oblique toppling however, 47% of the intersections were critical. As demonstrated in Figure 6(d), Set 1 is the most critical joint set for flexural toppling and this mode of failure is deemed to be of most importance in slope stability in this bench area. Pre-split blasting to re-profile parts of this slope is described in Keverne *et. al.,* 2015.

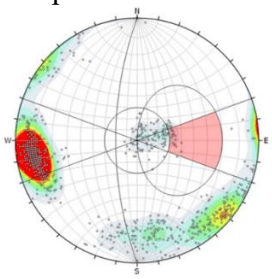

6 (a) Planar failure

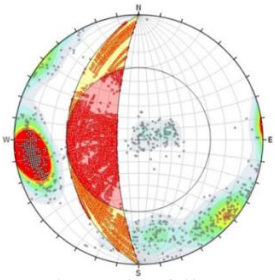

6(b) Wedge failure

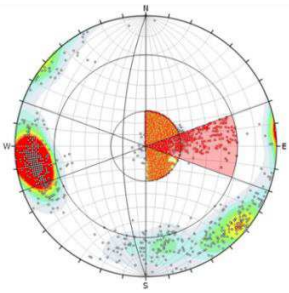

6(c) Direct toppling

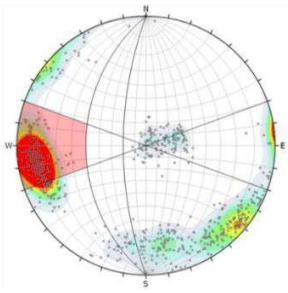

6 (d) Flexural toppling

	Critical	Total	%
Direct toppling (intersection)	16451	316180	5.2
Oblique toppling (intersection)	148110	316180	46.8
Base plane (all)	96	796	12.1
Base plane (set 4)	57	63	90.5

	Critical	Total	%
Flexural toppling (All)	327	796	41.1
Flexural toppling (Set 1)	296	304	97.4

Figure 6. Kinematic analysis of East face of Melbur Pit.

3 THERMAL INFRARED IMAGING

Objects at a temperature of less than 500 °C emit thermal radiation in the infrared spectrum. Thermography is a Non-Destructive Testing (NDT) technique in which temperature changes on the surface of rock exposures can be used to assess underlying conditions and interior discontinuities in some cases. Radiometric images or thermograms can be generated by a thermal imager in the infrared (IR) band, roughly 9,000–14,000 nanometers. When rock is loaded, the thermal infrared radiation of the rock surface changes.

3.1 *Previous work linking TIR studies with geomechanics*

McHugh and Girard (2002) investigated thermal imaging to distinguish geomechanical structure in mining environments. They considered that the differential cooling as a result of water saturation levels and flows in wall rocks have the potential to map geologic faults, contacts, and altered zones. Temperatures are greater in high-stress areas than low-stress areas and according to Liu et al, 2011 tension fractures appear as temperature-decrease anomalies. They determined that a thermal imager could detect a loose rock block in a mine tunnel. The same authors presented the results of infrared imaging of a slope in an opencast mine. Two lower temperature areas correlated with a compressive zone and a fault separated by a higher temperature zone between them. Although this may seem counter-intuitive, they postulated that fractured rock in the two areas contained more water so the temperature in the fault and the compressive zone are lower.

The infrared thermograms obtained by Martino and Mazzanti (2013) identified positive and negative anomalies in the temperature variations which corresponded to joint sets and discontinuities within the face of the slope. Thermal imaging was used in slope stability analysis and the implications of ground water in the slope face were assessed by Zwissler (2013). Due to the instability of the cliffs, no invasive soil sampling or testing was performed on the cliffs, however thermal imagery was used in the assessment of ground water. The FLIR thermal IR imaging indicated a band of lower temperature with respect to the temperature of the surrounding soil, which was associated with moisture (Zwissler (2013)).

3.2 *TIR imaging within china clay pits*

The aim was to investigate the changes in temperature in a bench section of a china clay pit. Data was collected and images taken during June and July 2014. The thermographic images were created using a FLIR ThermaCAM$_{TM}$ B2. 3-D laser scans obtained from the same location were merged with both infrared and digital photographic images using Cyclone 9 software and Photoshop. To correct the target pit face temperature, the IR camera software required inputs for the emissivity of the object, atmospheric attenuation and temperature, and temperature of the ambient surroundings. The emissivity value was standardised at 0.82 for the granite as the surface was rough and weathered (Danov *et al*., 2007). Batch photographs were taken from the same location which allowed for an overlay/blending of the images afterwards. At each site the IR camera settings were altered with an approximate atmospheric temperature. The majority of the images were standardised within a temperature range of 8–19˚C based on measured temperatures of the ambient surroundings. Another method of calibration involves measuring the temperature of several points on the scanned object using a thermocouple. However, in remote monitoring situations this is not possible.

The IR camera was manually adjusted to focus on the required slope. The temperature range was also altered on site to provide a clearer representation of the slope; however, this was problematic later on in the process when collating the images due to the influence of the sun.

3D analysis of thermographs was also achieved by overlaying the thermal images onto point clouds of the same bench face position.

3.3 *Example results*

Figure 7 shows firstly, an example of overlapping the rectangular thermal images onto a digital photograph and secondly draping the thermal images onto a 3-D point cloud. The blue areas indicate colder zones which are postulated to be structures which, at some stage of their genesis, have been subject to alteration by fluids penetrating along lower stress discontinuities in the rock. These may still be conduits for groundwater flow. The advantage of draping thermal images over the point cloud is that the orientation of specific discontinuities can then be determined in Split FX. Several features of interest are noted on the images in Figure 8, numbered 1, 2 and 3.

1. A sub-horizontal discontinuity coloured blue in the infrared image, suggesting that moisture also infiltrated horizontally at this point.

2. Intersection of two discontinuities is clearly visible in an area devoid of shadow.

3. Major sub-vertical discontinuities striking perpendicular to the face are indicated by dark blue features in the infrared images. These correspond to Set 2 (blue) shown in Figure 3. From the mean pole of this set indicated in the major plane plot in Figure 6 and data in Table 3 the mean pole of this set is orientated at 77°/348°.

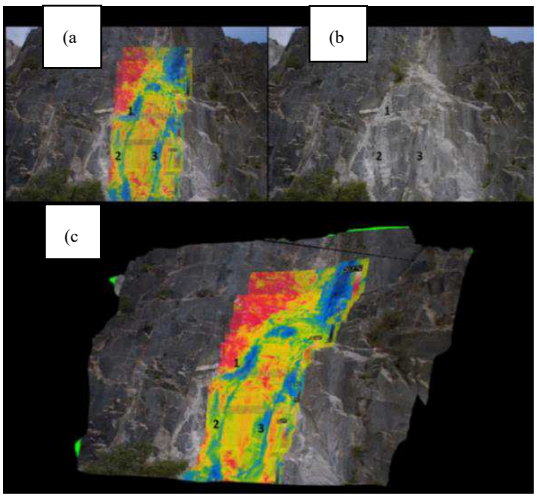

Figure 7. (a) 2D thermal overlay on RAW format digital image. (b) Digital RAW format photograph. (c) 3-D manipulation of thermal image draped over the point cloud. The numbering on the images represents key areas of interest explained in the text above.

Figure 7 also demonstrates that surfaces of discontinuities that have been subject to alteration have a different thermal response to unaltered rock faces. The highly kaolinized zone to the left hand side of the thermograms in Figure 8(a), indicated by numbers 2 and 4, is characterized by dark blue coloured thermographic imaging indicating the lowest temperatures equating to approximately 8°C. The orientation of this particular highly kaolinized discontinuity surface corresponds to Set 4 (orange) in Figure 3. In Table 2 the mean orientation of this major joint set in this section of the bench is seen to be 86°/310°.

Figure 8. (a) Thermal images draped over point cloud of same position depicted in figures 6 and 10 (b) Raw format digital image of same exposure aids identification of specific features.

4 CONCLUSIONS

This preliminary study of combined remote methods produced promising results. The results of 3-D laser scanning provided input data for kinematic slope stability analysis. In more conventional scan-line mapping of a single section carried out by geotechnical personnel, a bias occurs in the mapped discontinuity orientation data depending on the orientation of the scanline, hence it is recommended that three orthogonal scans be carried out. The effect of scanline direction with respect to particular discontinuity orientations is different for 3-D laser scanning but a bias still occurs. In order to obtain a more representative sample of joint at least two orthogonal faces were scanned in each pit and this will be explored in a further paper. In addition, for each exposure, scans were obtained from several different orientations to reduce occlusion.

For this research patches and traces were fitted individually in Split-FX rather than automatically. Images obtained from Terrestrial Infrared (TIR) imaging, combined with 3-D laser scans were used to identify particular joint orientations associated with alteration/fluid flow. Ideally future work should be undertaken using a 3-D laser scanner which incorporates a thermal camera which would avoid any errors in fitting the digital and laser images together. Zones where no patches could be fitted to the point cloud in Split-FX corresponded mostly with the wider kaolinized zones where the joints have been obliterated by the process of kaolinization. Using infrared thermal imaging the kaolinized zones in the slope were not only identifiable due to the low temperature profiles but the more precise positions of altered zones were identifiable within areas covered with superficial coating of washed out clay. The clear depiction of vegetation in thermograms is an issue however in that underlying discontinuities are obscured meaning that only clean faces can be fully analysed using thermography.

Kinematic analyses can be carried out using actual slope angles and directions in critical zones rather than representative values. Orientation of kaolinized zones can be determined using the combined thermal IR (TIR) images draped onto the 3-D laser scans. This research has demonstrated the potential use of combined remote methods for slope characterization, understanding of groundwater flow and mineralogical recognition.

5 ACKNOWLEDGEMENTS

Application of remote technology for data capture leading to improved rock mass characterization is part of research within the STOICISM project. The STOICISM research project has been supported by the European Commission under the 7th Framework Programme through the grant number 310645.

6 REFERENCES

Bristow and Exley, 1994. Historical and geological aspects of china clay industry of southwest England. Transactions of the Royal Geological Society of Cornwall, 21 (1994): 247–314.

Cyclone 9 software. 2014. *http://www.leica-geosystems.com/en/hds-software-leica-cyclone_6515.htm*

Danov, M., Petkov, D., Tsanev, V. 2007. 'Investigation of thermal infrared emissivity spectra of mineral and rock samples'. New developments and challenges in remote sensing. http://www.gbv.de/dms/tib-ub-hannover/531900762.pdf

Dips 6, Rocscience. 2006. Structural data processing software, Toronto. *http://www.rocscience.com/products/1/Dips*

FLIR Quick report software. *http://www.flir.co.uk/instruments/display/?id=60093*

Health and Saftety Executive. 2013. Health and safety at quarries. The Quarries Regulations 1999. Approved Code of Practice ISBN: 9780717663354

Keverne, B., Howe, J., Pascoe, D., Eyre, M., Coggan, J. 2015. 'Remediation of a hazardous legacy slope face using pre-split blasting' Eurock 2015. In preparation

Liu, S., Xu, Z., Wu, L., Ma, B., Liu, X. 2011. 'Infrared Imaging Detection of hidden dangers in mining engineering'. Progress in Electromagnetics research symposium proceedings.

Manning, D.A.C., Hill, P.I. & Howe, J.H. 1996. 'Primary lithological variation in the kaolinized St Austell Granite, Cornwall, England'. *J. of the Geological Society*, London, 153: 827-838.

Martino, S., Mazzanti, P. 2013 .Integrating geomechanical surveys and remote sensing for sea cliff slope stability analysis: the Mt. Pucci case study (Italy). Natural hazards and earth system sciences. 14: 831-848.

McHugh, E.L., Girard, J.M. 2002. Evaluating techniques for monitoring rock falls and slope stability.

Psyrillos, A. Manning, D.A.C. & Burley, S.D. 1998. 'Geochemical constraints on kaolinization in the St Austell granite, Cornwall, England. *Journal of the Geological Society*. 155: 829-840

Split-FX 64. Split Engineering. 2013. Version 2.1.0 *http://www.spliteng.com/products/split-fx-software/*

Stead D, Coggan JS, Howe JH. 2000. Engineering geology and hazard assessment of excavated china clay slopes, Geoscience in South West England, 10, PT 1 2000 (10): 72-76.

Sturzenegger, M. and Stead D. 2009. 'Close-range terrestrial digital photogrammetry and terrestrial laser scanning for discontinuity characterization on rock cuts'. *Engineering Geology*, Volume 106, Issues 3–4, 12 June 2009: 163-182

Zwissler, B.E. 2013. 'A study of the thermal impacts of freeze-thaw on cliff recession at the Calvert Cliffs in Calvert County, Maryland'. Michigan Technological University.